Atmos. Chem. Phys. Discuss., 13, 5509–5552, 2013
www.atmos-chem-phys-discuss.net/13/5509/2013/
doi:10.5194/acpd-13-5509-2013

Atmospheric Chemistry and Physics Discussions

Formation of aqueous-phase α-hydroxyhydroperoxides (α-HHP): potential atmospheric impacts

R. Zhao[1], A. K. Y. Lee[1], R. Soong[2], A. J. Simpson[2], and J. P. D. Abbatt[1]

[1]Department of Chemistry, University of Toronto, Toronto, ON, Canada
[2]Environmental NMR Centre, University of Toronto, Toronto, ON, Canada

Received: 12 February 2013 – Accepted: 13 February 2013 – Published: 27 February 2013

Correspondence to: J. P. D. Abbatt (jabbatt@chem.utoronto.ca)

Published by Copernicus Publications on behalf of the European Geosciences Union.

Abstract

The focus of this work is on quantifying the degree of the aqueous-phase formation of α-hydroxyhydroperoxides (α-HHPs) via reversible nucleophilic addition of H_2O_2 to aldehydes. Formation of this class of highly oxygenated organic hydroperoxides represents a poorly characterized aqueous-phase processing pathway that may lead to enhanced SOA formation and aerosol toxicity. Specifically, the equilibrium constants of α-HHP formation have been determined using proton nuclear resonance (^{1}H NMR) spectroscopy and proton transfer reaction mass spectrometry (PTR-MS). Significant α-HHP formation was observed from formaldehyde, acetaldehyde, propionaldehyde, glycolaldehyde, glyoxylic acid, methylglyoxal, but not from methacrolein and ketones. Low temperatures enhanced the formation of α-HHPs but slowed their formation rates. High inorganic salt concentrations shifted the equilibria toward the hydrated form of the aldehydes and slightly suppressed α-HHP formation. Using the experimental equilibrium constants, we predict the equilibrium concentration of α-HHPs to be in the µM level in cloud water but may be present in the mM level in aerosol liquid water (ALW), where the concentrations of H_2O_2 and aldehydes can be high. Formation of α-HHPs in ALW may significantly affect the effective Henry's law constants of H_2O_2 and aldehydes but may not affect their gas-phase levels. The photochemistry and reactivity of this class of atmospheric species have not been studied.

1 Introduction

Recent studies have shown that organic peroxides can be a significant portion of secondary organic aerosol (SOA) (Bonn et al., 2004; Docherty et al., 2005; Kroll and Seinfeld, 2008). Besides their contribution to SOA, organic peroxides also damage plant leaves (Polle and Junkermann, 1994), contribute to acid precipitation by oxidizing SO_2 to H_2SO_4 in the aqueous phase (Lind et al., 1987), and regenerate OH radicals (Matthews et al., 2005; Monod et al., 2007; Roehl et al., 2007; Kamboures et al.,

2010). α-Hydroxyhydroperoxides (α-HHPs) constitute a class of organic peroxide that has been observed in ambient air (He et al., 2010), rain water (Hellpointner and Gab, 1989; Sauer et al., 1996), and cloud water (Sauer et al., 1996; Valverde-Canossa et al., 2005), as reviewed by Hewitt and Kok (1991) and Lee et al. (2000).

Despite their observation in the atmosphere, our understanding of the formation mechanisms of α-HHP is still incomplete. It has been suggested that the recombination reaction of peroxy radical (RO_2) and hydroperoxy radical (HO_2), which is the major formation of organic hydroperoxides in gas phase, may not be a major formation pathway for α-HHPs (Carter et al., 1979; Atkinson 1990; Gab et al., 1995). Instead, other formation pathways, including aqueous-phase reactions have been proposed (Fig. 1). The first formation pathway, herein referred to as the Criegee Pathway, involves hydrolysis of the stabilized Criegee Intermediate (SCI) generated during alkene ozonolysis (Lee et al., 2000; Hasson et al., 2003; Ziemann and Atkinson, 2012). The second pathway involves reversible nucleophilic addition of H_2O_2 to carbonyls and is herein referred to as the Carbonyl Pathway (Hellpointner and Gab, 1989; Zhou and Lee, 1992). The Criegee Pathway has gained the majority of attention because α-HHPs have been observed from chamber ozonolysis of a variety of alkenes and monoterpenes (Hewitt and Kok, 1991; Neeb et al., 1997; Sauer et al., 1999; Hasson et al., 2001; Hasson and Paulson, 2003; Wang et al., 2012). This reaction pathway occurs in both the gas and aqueous phases but a few studies (Gab et al., 1995; Chen et al., 2008; Wang et al., 2012) have shown that aqueous-phase ozonolysis may lead to more efficient formation of α-HHPs compared to their gas-phase counterparts. In these studies, however, α-HHPs formed in the aqueous phase dominantly decomposed to H_2O_2 and aldehydes when analyzed under dilute conditions. The observed rapid decomposition of α-HHPs in such laboratory experiments has lead to a general perception that α-HHPs are unstable, and are merely a class of intermediates in the formation of carbonyls and H_2O_2 during ozonolysis.

However, recent studies have observed significant α-HHP formation upon the addition of H_2O_2 to aqueous solutions of dicarbonyls (Lee et al., 2011; Zhao et al., 2012)

and laboratory SOA extract (Liu et al., 2012) using advanced mass spectrometric techniques. Specifically, in our previous work (Zhao et al., 2012), α-HHP formation from glyoxal and methylglyoxal with H_2O_2 was monitored using an iodide (I^-) chemical ionization mass spectrometer coupled to a heated inlet line (Aerosol CIMS). This technique enabled the direct detection and characterization of α-HHPs using online mass spectrometry. In particular, the formation of α-HHPs from glyoxal and methylglyoxal was observed to be fast and reversible, with equilibrium constants between 40 and 200 M^{-1} for both compounds. As described below, an equilibrium constant of this magnitude suggests that α-HHPs could be formed in significant concentrations in aerosol liquid water (ALW) if aldehyde and H_2O_2 concentrations are high (Arellanes et al., 2006; Volkamer et al., 2009; Lim et al., 2010). However, the quantification using Aerosol CIMS is potentially complicated by thermodecomposition of α-HHPs and unknown processes involving droplet evaporation in the heated inlet, giving rise to the need for a more quantitative study using alternative techniques.

We note that although the Carbonyl Pathway is rarely discussed in the atmospheric chemistry literature, it has been studied somewhat in the 1940's and 50's by physical organic chemists using high precursor concentrations. For example, the formation of α-HHPs has been observed from several aldehydes (Satterfield and Case, 1954; Sander and Jencks, 1968) and ketones (Milas and Golubovic, 1959a,b). We also note that a closely related particle phase-reaction, peroxyhemiacetal formation (Fig. 1, pathway 3), which involves nucleophilic addition of an organic hydroperoxide to an aldehyde, has been previously proposed. (Tobias and Ziemann, 2000). Now, small carbonyls are gaining attention as potential SOA precursors via aqueous-phase processing (Ervens et al., 2011). The formation of α-HHP via the Carbonyl Pathway may provide an additional mechanism of processing of such carbonyls in the atmospheric aqueous phase. As well, the formation of α-HHP may also have significance to laboratory photooxidation experiments, where H_2O_2 is commonly used as a precursor for OH radicals.

Given that the potential of many carbonyls to form α-HHPs is currently unknown, the specific goals of this work were to experimentally determine the equilibrium con-

stants of α-HHP formation via the Carbonyl Pathway from a range of atmospherically relevant carbonyl compounds using two separate analytical methods: proton nuclear magnetic resonance (^{1}H NMR) spectroscopy and proton transfer reaction mass spectrometry (PTR-MS). ^{1}H NMR spectroscopy directly quantifies the chemical changes in the aqueous phase when a carbonyl is mixed with H_2O_2, and is particularly well suited for the investigation of thermodynamic equilibria. On the other hand, online PTR-MS measurement of the gas-phase concentration of carbonyls after addition of H_2O_2 provides better insight into the kinetics of the reactions and can assess the impact of α-HHP formation on the effective Henry's law constants (K_{Heff}) of the carbonyls. We note that thermodynamic information of the type derived in this paper is required to quantify the importance of different derivative organics in aerosol and cloud water, and yet it is frequently missing from the literature. The paper concludes with an assessment of the atmospheric importance of α-HHP formation by the Carbonyl Pathway.

2 Experimental

2.1 ^{1}H NMR measurements

The formation of α-HHPs from a suite of atmospherically relevant carbonyl species has been studied: formaldehyde (Sigma Aldrich, 37 wt % in water with 10–15 % methanol as stabilizer), acetaldehyde (Sigma Aldrich, > 99.5 %), propionaldehyde (Sigma Aldrich, < 97 %), glycolaldehyde (Sigma Aldrich, in solid dimer form), glyoxal (Sigma Aldrich, 40 wt % in H_2O), methylglyoxal (Sigma Aldrich, 40 wt % in H_2O), glyoxylic acid (Sigma Aldrich, 50 wt % in H_2O), methacrolein (Sigma Aldrich, 95 %), methylethyl ketone (ACP Chemicals Inc., 99 %), and acetone (EMD, 99.8 %) These compounds have low molecular weights, and exist largely in the gas phase. However, several compounds (e.g. glyoxal, methylglyoxal, glyoxylic acid and glycolaldehyde) are quite water soluble and can be important aqueous-phase SOA precursors (Carlton et al., 2007; Altieri et al., 2008; Perri et al., 2009; Ervens and Volkamer, 2010; Lim

et al., 2010; Tan et al., 2010; Ervens et al., 2011; Lee et al., 2011; Ortiz-Montalvo et al., 2012; Zhao et al., 2012).

Aqueous solutions (10 mM) of a targeted carbonyl were prepared individually from the commercial standards mentioned above. A known concentration (0.5 mM) of dimethylsulfoxide (DMSO, Fisher Scientific, 99.9 %) was added as an internal standard to assist the quantification and chemical shift calibration. A portion of commercial H_2O_2 stock solution (Sigma Aldrich, 30 % in water) was also added to the carbonyl solutions shortly after they were prepared at concentrations usually between 8.9 and 20 mM, but up to 100 mM for ketones and methacrolein due to insignificant α-HHP formation from these species. A 500 µL aliquot of the mixed solution was transferred into a 500 µL glass NMR tube along with 25 µL of D_2O (Cambridge Isotope Laboratories, Inc., 99.96 %) as a lock reagent for the ^{1}H NMR measurement. Using an auto-sampler (Bruker B-ACS 120) ^{1}H NMR spectra were acquired with a Bruker Avance 500 MHz spectrometer using a ^{1}H, ^{19}F, ^{13}C, ^{15}N 5 mm quadruple resonance inverse (QXI) probe fitted with an actively shielded Z gradient. ^{1}H NMR experiments were performed with presaturation using relaxation gradients and echoes (PURGE) (Simpson and Brown, 2005) water suppression and 128 scans, a recycle delay of 3 s, and 16 K time domain points. Spectra were apodized through multiplication with an exponential decay corresponding to 0.3 Hz line broadening in the transformed spectrum and a zero filling factor of 2, then manually phased and calibrated to the DMSO at 2.5 ppm. Spectral predictions were performed in Advanced Chemistry Development's ACD/SpecManager using a Neural Network Prediction algorithm (version 12.5). All calculations were performed using water as the solvent with a spectral line shape 2 Hz chosen to match those of the real datasets as closely as possible.

For most of the samples, the ^{1}H NMR spectra were taken within 24 h after the samples were prepared, and within 48 h for a small number of samples. The time scale of α-HHP equilibration is 30 to 60 min (confirmed in the PTR-MS experiments), so that the equilibria should be fully established when ^{1}H NMR spectra were taken. The sample solutions were no longer protected from room light once loaded on the auto-

sampler. To examine potential evaporation of carbonyls and OH generation from H_2O_2 photolysis, some methacrolein samples were analyzed a second time 10 h after the first measurement. Methacrolein was chosen because it is the most volatile aldehyde studied here (Allen et al., 1998) and is highly reactive to OH radicals (Herrmann et al., 2010) The concentration of methacrolein did not show observable change before and after 10 h of room light exposure, and so it is assumed that evaporative loss and room light exposure induced negligible effects to other samples as well.

The temperature inside the NMR instrument was controlled at 25 °C. A NMR tube typically stayed inside the instrument for 20 min for the homogenization of its magnetic field before the spectra were acquired. Water blanks and control experiments were performed to ensure that the peaks in the spectra are not from H_2O_2 reacting with water impurities or DMSO. The effect of pH was not examined. Previous studies reported that acid can catalyze the rate of α-HHP formation and decomposition but does not affect the equilibria (Marklund, 1971; Zhou and Lee, 1992).

2.2 Effects of inorganic salts

Aerosol liquid water (ALW) can contain high concentration of inorganic salts up to and beyond their saturation concentrations (Tang et al., 1997) making it important to investigate the effect of high concentrations of aqueous-phase inorganic salts on the equilibria. To do this, 1 M of either $(NH_4)_2SO_4$ (AS) or Na_2SO_4 (SS) was added to a number of acetaldehyde and glycolaldehyde samples. The NMR probe used in the current method is not compatible with any higher salt concentrations. The salts were added after the α-HHP equilibrium had been fully established.

2.3 PTR-MS measurements

To confirm the equilibrium constants determined by ^{1}H NMR spectroscopy and further investigate the effects of these condensed-phase equilibria to the K_{Heff} of the carbonyls, a setup involving a bubbler and a PTR-MS (Ionicon Inc., quadruple mass spectrometer)

was used, as shown in Fig. 2. This system was used to measure the effect on a carbonyl vapour pressure arising from the addition of H_2O_2.

Ultra pure N_2 (BOC Linde, grade 4.8) was introduced to a temperature-controlled glass bubbler containing an aqueous solution (10 mM) of a carbonyl compound. The gas phase carbonyl loading exiting the bubbler was measured by the PTR-MS after dilution (2 to 3 lpm) with ultra pure N_2. The bubbler was placed in dark during experiments to minimize light exposure. Teflon lines and connections were used downstream of the bubbler to minimize surface reactions and loss of carbonyls. N_2 was continuously introduced through the carbonyl solution until a stable PTR-MS signal was achieved at the mass-to-charge ratio (m/z) of the protonated carbonyl. A known concentration of H_2O_2 (typically 8.9 to 17.7 mM) was then added to the bubbler, and the N_2 flow was resumed until the PTR-MS signal reached a new equilibrium. Equilibrium constants were determined from the difference of the carbonyl signals detected before and after the H_2O_2 injection. With the detection limit set by the PTR-MS, this approach could be used only for sufficiently volatile carbonyls: acetaldehyde, propionaldehyde, methacrolein, methylethyl ketone and acetone. The experiments were typically performed at 25 °C except for those with acetaldehyde reaction giving rise to the formation of 1-hydroxyethyl hydroperoxide (1-HEHP), which were also conducted at 15 °C and 5 °C.

2.4 Reversibility test: addition of catalase

In both the NMR and PTR-MS experiments, catalase from bovine liver was added to the reaction mixture to react away H_2O_2 to test the reversibility of the reaction. In our previous study (Zhao et al., 2012), quenching of H_2O_2 led to the decomposition of α-HHPs and regeneration of the original aldehydes. For the ^{1}H NMR experiments, 1 µL of the catalase solution (Sigma Aldrich, 34 mg protein mL^{-1}) was added to 1 mL of the carbonyl-H_2O_2 reaction mixtures after the equilibrium was fully established. Control experiments were performed to confirm that there was no contribution of catalase to the ^{1}H NMR spectra. For the PTR-MS experiments, one drop of catalase was added to the 25 mL reaction mixture after the equilibrium was fully established. The N_2 flow

was resumed after the catalase addition, and the change of the carbonyl signals was monitored. Control experiments demonstrated that catalase did not cause any change in the PTR-MS signal at the *m/z* of interest.

3 Results and discussion

3.1 ^{1}H NMR results

With the exclusion of methacrolein, significant changes in the ^{1}H NMR spectra were observed for all the aldehydes upon addition of H_2O_2 to the carbonyl solution, with the magnitude of the change increasing with the concentration of H_2O_2. The reactions were also observed to be largely reversible from the catalase addition experiments. As described below, the formation of α-HHP from acetone and methylethyl ketone was observed to be minor. Spectral assignment was based on comparison to standards, manual interpretation and confirmed with spectral prediction.

The experiment involving acetaldehyde is shown in Fig. 3 as an example. Before the addition of H_2O_2, acetaldehyde and its hydrated gem-diol coexist in the solution (Fig. 3a). Based on their chemical shift and splitting patterns, the identities of the peaks are assigned and labeled. After addition of 17.7 mM of H_2O_2 (Fig. 3b), two new peaks appeared at chemical shifts 5.06 and 1.06 ppm, respectively, corresponding to the V and VI protons in 1-HEHP. It is not surprising that the two new peaks appeared very close to the peaks of hydrated acetaldehyde (i.e. the III and IV protons), given the similar structure between hydrated acetaldehyde and 1-HEHP. The reversibility of the reaction was confirmed upon addition of catalase (Fig. 3c), with the spectra then resembling those at the start of the experiment.

The water peak was very large in each spectrum even with the water suppression procedures, so that some overlapping analyte peaks complicated their peak assignment and quantification. For peaks partially overlapping with water (e.g. at 5.04 ppm in Fig. 3), baseline corrections were performed before quantification. Also, we note

that the gain of each NMR spectrum was auto-adjusted by the instrument so that the quantification of compounds had to be conducted by comparing the analytes' peak area and number of protons (#H) with signals arising from 0.5 mM of DMSO added as the internal standard. The calculation was performed in the following manner (Wallace 1984):

$$\frac{\text{Concentration of analyte (M)}}{\text{Concentration of Internal Standard (M)}} = \frac{\text{Peak area of analyte}}{\text{Peak area of internal standard}} \times \frac{\#\,\text{H}_{\text{internal standard}}}{\#\,\text{H}_{\text{analyte}}} \quad (1)$$

Based on the quantified concentrations, we calculated three equilibrium constants: the hydration equilibrium constant (K_{hyd}), equilibrium constant for α-HHP formation (K_{eq}), and the apparent equilibrium constant for α-HHP formation (K_{app}). The relationship between the three constants is illustrated in Fig. 4, and their definitions are below:

$$K_{hyd} = \frac{[\text{Carbonyl}_{hyd}]\text{eq}}{[\text{Carbonyl}_{non\text{-}hyd}]\,\text{eq}} \quad (2)$$

$$K_{eq} = \frac{[\alpha - \text{HHP}]\,\text{eq}}{[\text{H}_2\text{O}_2]\,\text{eq} \times [\text{Carbonyl}_{non\text{-}hyd}]\,\text{eq}} \quad (3)$$

$$K_{app} = \frac{[\text{Total } \alpha - \text{HHP}]\,\text{eq}}{[\text{H}_2\text{O}_2]\,\text{eq} \times [\text{Total Carbonyl}]\,\text{eq}} \quad (4)$$

where $[\text{Carbonyl}_{hyd}]$eq and $[\text{Carbonyl}_{non\text{-}hyd}]$eq represent the equilibrium concentrations of the hydrated form and the non-hydrated form of a carbonyl, respectively. The hydration equilibria of many atmospherically relevant carbonyls are well studied, and so, comparing our results to the literature values is a good way to verify our ^{1}H NMR method. In Eq. (3), [α-HHP]eq and $[\text{H}_2\text{O}_2]$eq represent the equilibrium concentrations of an α-HHP and H_2O_2. The usefulness of the K_{eq} defined this way is, however, limited

especially for dicarbonyls such as methylglyoxal that can form multiple α-HHP equilibria. Unambiguous determination of all the K_{eq} values is also impossible because some of the peaks are missing due to overlap with the water peak. K_{app}, on the other hand, is a better indicator for the overall potential of α-HHP formation from each carbonyl compound. The [Total α-HHP]eq and [Total Carbonyl]eq in Eq. (4) represent the summed equilibrium concentrations of α-HHPs and carbonyls (i.e. hydrated and non-hydrated forms), respectively. Given that the K_{hyd} values did not change with the H_2O_2 addition, [Total Carbonyl]eq can be estimated from determination of the concentration of either the hydrated or non-hydrated form of the carbonyl. Thus the use of K_{app} negates the need for unambiguous quantification of all the peaks. The measured K_{hyd} and K_{app} values of the carbonyls using ^{1}H NMR are tabulated in Tables 1 and 2, respectively, along with values from the literature.

3.2 PTR-MS results

Acetaldehyde, propionaldehyde, methacrolein, acetone and methylethyl ketone were detected in their protonated form at *m/z* 45, 59, 71, 59 and 73, respectively. Besides their protonated molecular ions, three other major fragment ions at *m/z* 31, 39 and 49 were detected from propionaldehyde, and one major fragment ion at *m/z* 55 was detected from methylethyl ketone. For these two carbonyls, the total signal intensity of the protonated molecular ion and the major fragments were used for quantification. No α-HHP signal was detected using the current PTR-MS method.

Figure 5 illustrates data from a sample experiment for acetaldehyde at 25 °C. Acetaldehyde signal normalized to the H_3O^+ reagent ion became stable 20 min after a 10 mM solution was placed in the bubbler at time (i). After 17.7 mM of H_2O_2 was injected to the solution at time (ii), the acetaldehyde signal decreased and rapidly reached a new equilibrium due to the formation of 1-HEHP in the solution. Upon addition of catalase at time (iii), the acetaldehyde signal recovered close to its original

level. A similar trend was observed for propionaldehyde, but methacrolein, acetone and methylethyl ketone did not show any observable change upon H_2O_2 addition.

The equilibrium constants of α-HHP formation from acetaldehyde and propionaldehyde were calculated from the difference in their signals before and after H_2O_2 addition (Table 2). The K_{app} values defined in Eq. (4) are calculated by using the aldehyde signal after the H_2O_2 addition as [Total Carbonyl]eq, the magnitude of change in the aldehyde signal as [Total α-HHP]eq, and the difference between the total H_2O_2 concentration and [Total α-HHP]eq as [H_2O_2]eq. The calculation of K_{app} here is based on assumptions that: (1) the non-hydrated forms of acetaldehyde and propionaldehyde detected by the PTR-MS are proportional to their total concentrations in the solution (i.e. their K_{hyd} values remain constant), and (2) their signal change is solely due to α-HHP formation. The first assumption is verified by the observation from the ^{1}H NMR experiments that K_{hyd} values stayed constant regardless of the amount of H_2O_2 addition.

The validity of the second assumption is challenged by irreversible processes potentially occurring in the system, such as oxidation reactions induced by H_2O_2 and volatilizational loss of the aldehydes due to bubbling. To examine formation of irreversible products, particularly organic acids, the PTR-MS was operated under the scan mode (*m/z* 20 to 120) but no change was observed in the mass spectra aside from the decay of the protonated molecular ion and major fragments. As well, the recovery of acetaldehyde and propionaldehyde were observed to be 96 and 85 %, respectively (Table 2). The high recovery illustrates that the reaction is mostly reversible due to α-HHP formation. The volatilizational loss of acetaldehyde and propionaldehyde from pure solutions at 25 °C over two hours of bubbling could be up to 11 and 14 %, based on the flow rate of N_2 through the bubbler, the solution volume, concentration and the Henry's law constants (K_H) of the two aldehydes.

3.3 Comparison of equilibrium constants

In general, the K_{hyd} values showed good agreement with literature values (Table 1) and the K_{app} values determined from the two methods reasonably agreed with each other and with the literature (Table 2). The inability of methacrolein, acetone and methylethyl ketone to form α-HHP was confirmed from both methods. Formic acid formation was observed upon H_2O_2 addition to methylglyoxal and glyoxylic acid. Detailed discussion of results for each compound is provided below, and an example ^{1}H NMR spectra for each compound is provided in the Supplement.

3.3.1 Formaldehyde

The equilibrium concentration of formaldehyde was calculated by subtracting the amount of hydroxymethyl hydroperoxide (HMP) observed (Fig. 6, proton III) from the total concentration of 10 mM. In particular, the K_{hyd} of formaldehyde is so large that the aldehydic proton peak (proton I) was below the ^{1}H NMR detection limit which is determined to be approximately 100 µM. This observation is supported by the large K_{hyd} value in the literature: 2.3×10^3 (Betterton and Hoffmann, 1988). The hydrated formaldehyde proton (II) was also not observed in the ^{1}H NMR spectra likely due to overlap with the water peak.

We propose that the small peak that appeared at 4.94 ppm is due to formation of bis-hydroxymethyl hydroperoxide (BHMP, proton IV). This peroxyhemiacetal compound forms by HMP further reacting with non-hydrated formaldehyde. BHMP has been observed in a number of laboratory studies (Marklund, 1971; Zhou and Lee, 1992; Gab et al., 1995) and in the atmosphere (He et al., 2010). The K_{app} for BHMP formation ($K_{app,BHMP}$) is calculated by Eq. (5):

$$K_{app,\,BHMP} = \frac{[BHMP]eq}{[HMP]eq \times [Total\ Carbonyl]eq} \quad (5)$$

to be $12.0 \pm 1.3\,M^{-1}$ (where the uncertainties are precisions derived from a number of replicates), showing excellent agreement with two reported values: $11.7\,M^{-1}$ from Zhou and Lee (1992) and $14.0\,M^{-1}$ from Marklund (1971).

The overall K_{app} value for formaldehyde is determined to be $164 \pm 31\,M^{-1}$. This value is slightly larger than the three literature values reported because those values are for only HMP formation, while the value in this work incorporates BHMP formation.

3.3.2 Acetaldehyde

The K_{hyd} value, 1.43 ± 0.04, agrees very well with the reported value (Greenzaid et al., 1967). Our measured value of K_{app}, $94.8 \pm 12.5\,M^{-1}$, is larger than the only literature value by a factor of 2 (Kooijman and Ghijsen, 1947). The results from the PTR-MS, $132 \pm 15\,M^{-1}$, showed reasonable agreement with the ^{1}H NMR results.

3.3.3 Propionaldehyde

The experimental K_{hyd} value, 1.26 ± 0.13 was slightly larger than the reported value 0.7 (Greenzaid et al., 1967). The agreement between the ^{1}H NMR and the PTR-MS measurements was fair, with the K_{app} value determined to be 51.1 ± 8.0 and $84 \pm 12\,M^{-1}$, respectively. The catalase recovery was 83 ± 3 and 85 %, respectively.

3.3.4 Glycolaldehyde

Glycolaldehyde solutions were prepared by dissolving glycolaldehyde dimer (2,5-dihydroxy-1,4-dioxane) in water. The major peaks in the ^{1}H NMR spectra were from glycolaldehyde monomers, indicating that monomerization proceeds almost to completion in the solution at the current concentration used (Yaylayan et al., 1998; Glushonok et al., 2000). The observed K_{hyd} value, 16.0 ± 1.3, fell into the same range as several other reported K_{hyd} values (Sorensen, 1972; Yaylayan et al., 1998). There are no prior reports of the equilibrium constant of α-HHP formation.

3.3.5 Methacrolein

Among the carbonyl compounds studied, methacrolein was the only aldehyde that did not show significant α-HHP formation, as confirmed by both the ^{1}H NMR and PTR-MS studies. The K_{app} was determined to be $0.8 \pm 0.7\,M^{-1}$ from the ^{1}H NMR, but no observable α-HHP formation was observed using PTR-MS. We propose that the carbonyl group and the C=C double bond in methacrolein form π-electron conjugation which stabilizes the aldehyde from nucleophilic attacks. Although Claeys et al. (2004) proposed a mechanism of polyol formation from methacrolein and H_2O_2 in the particle phase (Claeys et al., 2004), no such products were observed in the current experiment.

3.3.6 Glyoxal

No quantitative data for glyoxal could be acquired from the current study. In particular, the PTR-MS is not highly sensitive to glyoxal, and most of the glyoxal peaks in the ^{1}H NMR spectra were hidden behind the water peak. The only literature value for K_{app} of glyoxal is from our previous work (Zhao et al., 2012), where we estimated the lower limit of K_{app} to be $40\,M^{-1}$ using an Aerosol CIMS.

3.3.7 Methylglyoxal

Hydration and α-HHP formation occurring on one or both of the carbonyl groups in methylglyoxal would lead to a slightly different chemical environments for the protons, making the ^{1}H NMR spectra of methylglyoxal highly complicated. We performed peak assignment based on the predicted chemical shift of each proton by spectral prediction (see Sect. 2.1) and on changes in the peak intensity upon H_2O_2/catalase additions, but the peak assignment for methylglyoxal is associated with a higher level of uncertainty than with the other molecules. A non-negligible amount of formic acid formation was also observed with H_2O_2 addition (8.2 ppm, Fig. S2). Formic acid likely forms irreversibly, as shown by a decreasing trend in catalase recovery, 91, 87, and 84 %,

with increasing amount of H_2O_2 addition: 10, 15 and 20 mM. We assumed that formic acid formation was slow compared to the α-HHP formation equilibrium, so that K_{app} can still be calculated from the amount of α-HHP formed and methylglyoxal remaining. This way, the K_{app} value is determined to be $25 \pm 4\,M^{-1}$. This value falls below the range of our previous estimation: $40 \sim 200\,M^{-1}$ (Zhao et al., 2012). The discrepancy between the two studies may be explained either by the uncertainties associated with the Aerosol CIMS method (see Sect. 1), or by the methylglyoxal peak assignment here.

3.3.8 Glyoxylic acid

The ^{1}H NMR spectra of glyoxylic acid solutions indicates that it exists mostly in its hydrated form, qualitatively agreeing with its large reported K_{hyd} value (3×10^3, Sorensen et al., 1974). Upon H_2O_2 addition, significant amount of formic acid formation (8.1 ppm, Fig. S5), up to 50 % of the total glyoxylic acid, was observed. Irreversible formic acid formation from glyoxylic acid and H_2O_2 in the aqueous phase is well documented (Tan et al., 2009; Lee et al., 2011; Ortiz-Montalvo et al., 2012). We propose that at least some of the glyoxylic acid exists in its α-HHP form because the decay of glyoxylic acid was larger than the amount of formic acid formation, and some of glyoxylic acid was regenerated with catalase addition. However, a reliable quantification of the K_{app} value is highly challenging, as reflected by the large uncertainties in the reported value ($440 \pm 270\,M^{-1}$).

3.3.9 Acetone and methylethyl ketone

The two ketones studied did not exhibit significant α-HHP formation in either the ^{1}H NMR or the PTR-MS experiments. In general, ketones are known to be relatively stable against nucleophilic addition as compared to aldehydes. This is because the additional alkyl group stabilizes the carbonyl functional group via electron donation. Such a trend can be also seen from the small K_{hyd} reported for ketones (e.g. 0.002 for acetone, Bruice, 2004). The unstable nature of α-HHPs from ketones has also been reported

previously (Sauer et al., 1999; Wang et al., 2012). However, we note that these simple ketones do not fully represent the diversity of ketones in SOA. In fact, the current work and past studies have implied α-HHP formation on the ketone group of methylglyoxal (Stefan and Bolton, 1999; Zhao et al., 2012).

3.4 Temperature dependence of K_{app}

We observed enhanced 1-HEHP formation from acetaldehyde with decreasing temperature, but with slower reaction rates. Example data are shown in Fig. 7a. The ratio of acetaldehyde signal to its initial level at 5, 15 and 25 °C is plotted as a function of time. The injection of H_2O_2 (13.3 mM) was performed at time (i). The time required for equilibration was approximately 1, 2 and 5 h at the three temperatures. The signal level at equilibrium, determined by fitting an exponential function to the signal, decreases with decreasing temperature, as indicated by the horizontal dashed lines in Fig. 7a. The temperature dependence observed here implies more significant α-HHP formation at colder temperatures. The K_{app} values determined at the three temperatures are listed in Table 3. From a van't Hoff plot of these data (Fig. 7b), a positive slope was obtained corresponding to a standard enthalpy change ($\Delta H°$) of $-29.7 \pm 1.3\,kJ\,mol^{-1}$.

Since the equilibrium is reached slowly in the 15 and 5 °C experiments, we can estimate the rate coefficient of 1-HEHP formation by fitting an exponential curve to the decaying acetaldehyde signal and obtaining its slope at early reaction times where there is no reverse reaction occurring and the initial concentrations of acetaldehyde and H_2O_2 are known. Using this method, the second order rate constants of 1-HEHP formation were determined to be 0.012 ± 0.002 and $0.0045 \pm 0.0005\,M^{-1}\,s^{-1}$, respectively. The kinetics at 25 °C were too fast to be estimated. We note that the pH of the solution is not controlled in our experiment. Even though the equilibrium is independent of the solution pH, both the formation and decomposition rates of α-HHP have been reported to be pH dependent (Zhou and Lee, 1992).

3.5 Effects of inorganic salt addition

The results of the inorganic salt addition experiments are summarized in Table 4. We observed that the addition of AS and SS caused a small increase in K_{hyd} and a small decrease in K_{app} for both acetaldehyde and glycolaldehyde. To assess whether the differences are statistically significant, one tail t-tests were performed to make comparisons between the average K_{hyd} and K_{app} values with and without salt addition, and the p-values from the t-tests are listed in Table 4. P-values that are statistically significant at the 95 % confidence level (i.e. $p < 0.05$) are indicated with [a] in Table 4. All the equilibrium constants for glycolaldehyde and the K_{hyd} of acetaldehyde with AS addition have been determined to be statistically significant, whereas the other three values point in the same direction but with less statistical significance.

These observations qualitatively agree with Yu et al., who observed that addition of SS shifted the hydration equilibrium of glyoxal to the dihydrated form of the monomer (Yu et al., 2011). The enhancement of K_{hyd} and the suppression of K_{app} by SS and AS observed in the current study is likely arising from similar effects at the molecular level, especially those associated with SO_4^{2-}. The current observation implies that the inorganic effects may affect aqueous-phase equilibria of aldehydes in general. Yu et al. suggested that this effect might be more pronounced for aldehydic functional groups adjacent to an electron withdrawing group (e.g. glyoxal). Glycolaldehyde has an additional electron withdrawing hydroxyl group compared to acetaldehyde, which may explain why the inorganic salt effect appears to be larger for glycolaldehyde.

4 Atmospheric implications

With the first thorough assessment of the equilibrium constants for α-HHP formation, we can make initial assessments for the likely atmospheric significance for these compounds.

4.1 Equilibrium concentrations of α-HHPs in cloud water and aerosol liquid water

The amount of α-HHP formation via the Carbonyl Pathway in atmospheric aqueous phases is directly dependent on the abundance of the different reactants. Cloud/fog water and ALW are commonly considered as two qualitatively different reaction media (Volkamer et al., 2009; Ervens and Volkamer, 2010; Lim et al., 2010) due to orders of magnitude differences in their liquid water content (LWC), surface-to-volume ratio, and aqueous-phase reactant concentrations. The aldehyde species studied here span a wide range of water solubility. Specifically, the aqueous-phase concentrations of volatile species such as acetaldehyde, propionaldehyde and methacrolein, whose K_H values are typically below 20 M atm^{-1} (Zhou and Mopper, 1990; Allen et al., 1998), are expected to be low. However, aqueous-phase concentrations of highly water soluble aldehydes, such as glycolaldehyde, methylglyoxal and glyoxal can be substantial. In particular, the concentration of glyoxal can be up to hundreds of μM in polluted fog water (Carlton et al., 2007; Tan et al., 2009) and has been proposed to be present up to the molar level in ALW (Volkamer et al., 2009). As well, there are also studies suggesting that H_2O_2 concentration in ALW can also be unexpectedly high. Based on filter extracts of ambient aerosol and model calculations, Arellanes et al., suspected that H_2O_2 concentration in ALW might be up to 100 mM (Arellanes et al., 2006), although there is some possibility that the H_2O_2 that is detected has arisen from decomposition from other species or been formed post collection in such off-line analyses. The concentration of H_2O_2 in cloud water usually does not exceed 100 μM (Sakugawa et al., 1990).

Assuming an average K_{app} of 100 M^{-1}, which is approximately the middle point of the measured K_{app} values from the current study, we calculated the concentrations of α-HHPs that would be present with various equilibrium concentrations of H_2O_2 and total aldehyde (Fig. 8). Note that the effect of inorganic salts is not considered in this calculation but our studies suggest that these effects are likely to be minor relative

to the uncertainties in the assumed reactant concentrations. The simulation indicates that α-HHP formation in cloud water is unlikely to be significant, with its concentration not exceeding 10 μM even with the highest combination of reactant concentrations. In ALW, however, α-HHP concentrations may be comparable to that of H_2O_2. When the equilibrium concentrations of H_2O_2 and aldehydes reach 10 mM and 100 mM, their respective upper limits in ALW, 100 mM of α-HHPs may be formed.

4.2 Impact of α-HHP formation on the atmospheric partitioning of aldehydes and H_2O_2

The water solubility of α-HHP can be very high. The K_H has only been reported for one α-HHP, i.e. that from formaldehyde (HMP): 5×10^5 M atm^{-1} (Zhou and Lee, 1992) and 1.67×10^6 M atm^{-1} (O'Sullivan et al., 1996). These values are two orders of magnitude larger than that of formaldehyde and one order of magnitude larger than that of H_2O_2. This implies that the formation of α-HHP in the aqueous phase will enhance the K_{Heff} of aldehydes and/or H_2O_2:

$$K_{Heff,Ald} = K_{H,Ald}(1 + K_{app}[H_2O_2]_{aq}) \quad (6)$$

$$K_{Heff,H_2O_2} = K_{H,H_2O_2}(1 + K_{app}[\text{Total Aldehyde}]_{aq}) \quad (7)$$

The enhancement of K_{Heff} compared to K_H depends on the value of K_{app} and the amount of H_2O_2 or total aldehyde existing in the aqueous phase.

We simulated the partitioning of an initial mixing ratio of 1 ppb gas-phase aldehyde or H_2O_2 that is exposed to typical cloud water or ALW conditions, both with and without α-HHP formation (see Table 5). In particular, in the case of the aldehydes, we assume a fixed concentration of H_2O_2 in solution (as specified in Table 5), and in the case of H_2O_2 we assume a fixed concentration of dissolved total aldehydic functional group. The LWC is orders of magnitude higher in the cloud water scenario than with ALW, i.e. 1 g m^{-3} vs. 1 μg m^{-3}. By contrast, the equilibrium concentrations of total aldehyde and H_2O_2 are assumed to be much higher in the ALW case. The purpose of this simple

simulation is to assess how the enhancement of K_{Heff} arising from α-HHP formation leads to an associated alteration in the gas-aqueous phase partitioning of H_2O_2 and aldehydes based only on the thermodynamic equilibria of Henry's law partitioning and α-HHP formation. Kinetic issues, such as formation rate constants and mass transfer rates are not addressed, and we assume the HHPs are involatile. We again stress that the chemical concentrations in ALW is highly uncertain. The assumed concentrations here (i.e. 10 mM for H_2O_2 and 100 mM for total aldehyde) can be considered as their respective upper limits, and these calculations should be viewed as a simple modeling exercise to highlight potential atmospheric importance only. The simulation was performed for formaldehyde, acetaldehyde and H_2O_2, and the results are shown in Table 6.

Without α-HHP formation, the majority of formaldehyde and acetaldehyde exists in the gas phase under both scenarios, leaving their gas-phase mixing ratio essentially unaffected at 1 ppb. More than half of the H_2O_2 population will dissolve into the aqueous phase under the cloud water scenario due to its relatively high K_H, but the majority stays in the gas phase under the ALW scenario due to the small LWC. The measured K_{app} values for formaldehyde and acetaldehyde from the current work are used for the simulation of α-HHP formation. For the case of H_2O_2 simulation, an average K_{app} of $100\,M^{-1}$ was assumed.

The first conclusion from the simulation is that, in the ALW scenario, K_{Heff} values of H_2O_2 are enhanced by up to an order of magnitude relative to the K_H values when α-HHP formation occurs, while the enhancement in the cloud water scenario was minor. However, even with such large enhancement in the K_{Heff} values, the gas-phase mixing ratio of aldehydes and H_2O_2 are essentially unchanged from the case without α-HHP formation because of the low LWC. The K_{Heff} values for formaldehyde and acetaldehyde were also enhanced by over a factor of two in ALW when α-HHP formation occurs.

The second conclusion arises from the resulting α-HHP concentration in the aqueous phase. Particularly in the H_2O_2 simulation, by assuming a total aldehyde concen-

tration of 100 mM at equilibrium in the ALW scenario, approximately 0.7 mM of α-HHP forms in ALW. We raise the possibility that this high concentration of α-HHP may partially explain the surprisingly high concentrations of H_2O_2 previously observed from ambient aerosol (Hasson et al., 2003; Arellanes et al., 2006). As suggested by these workers, because of the dilution associated with ambient aerosol extraction, α-HHPs should completely decompose to H_2O_2 upon analysis, contributing to its high concentrations observed from the extract. Indeed, for this simulation, the concentration of the α-HHP present in solution is roughly an order of magnitude larger than the concentration of H_2O_2 in solution. The α-HHP concentrations in the formaldehyde and acetaldehyde simulations were all enhanced, but not nearly as much as the H_2O_2 simulation case.

Of course, these assumptions are highly dependent on the assumed concentration of aldehydic functional groups in ALW, and that they all participate in α-HHP formation with the assumed K_{app}. The degree to which such groups are present in ALW is poorly characterized, however it would be expected that fresh SOA, for example that formed by ozonolysis, will have these species present.

4.3 Other atmospheric implications

As mentioned previously, α-HHP can also form via the hydrolysis of SCI, i.e. the Criegee Pathway. If this reaction occurs in cloud water, the resultant α-HHP would most likely decompose to H_2O_2 and a corresponding carbonyl compound. However, if a hydrolysis reaction of SCI occurs in ALW, which is generally more concentrated than cloud water, the resulted α-HHP may not fully decompose given the α-HHP equilibria studied in the current work. If the α-HHP does decompose, the H_2O_2 generated from the decomposition of α-HHP may meet another aldehydic species with higher concentration (e.g. glyoxal) to form a different α-HHP.

As α-HHP concentration builds up in ALW, α-HHP themselves can act as nucleophiles and form peroxyhemiacetals by reacting with aldehydic functional groups (see Pathway 3 in Fig. 1), as in the case of BHMP formation from HMP and formaldehyde

(Sect. 3.3.1). This reaction of α-HHP is a specific mechanism of peroxyhemiacetal formation initially proposed by Ziemann and coworkers (Tobias and Ziemann, 2000; Docherty et al., 2005) and later confirmed by several recent laboratory studies (Hall and Johnston, 2012; Yee et al., 2012). The current study is an indication that H_2O_2 can undergo the analogous reaction.

Formation of such hydroxyl and hydroperoxyl functional groups reduces the vapor pressure of an organic compound substantially (Kroll and Seinfeld, 2008) and increases its solubility. It is possible that peroxyhemiacetals and α-HHPs can stay in the particle phase even after water evaporation and can thus be a pathway by which relatively volatile aldehydes are involved in SOA formation. Recently, Liu et al. (2012) observed that addition of H_2O_2 to the water extract of isoprene SOA caused significant increase in its degree of oxygenation and enhancement of its hygroscopicity. It is likely that the α-HHP and peroxyhemiacetals contributed to such physico-chemical changes of the SOA water extract. In fact, decay of carbonyls and significant formation of 1-HEHP were observed in their study.

The α-HHPs may also be photolyzed by actinic radiation, leading to the cleavage of the peroxide (O–O) bond and the regeneration of an OH radical (Monod et al., 2007; Roehl et al., 2007; Kamboures et al., 2010). It needs to be determined whether this process occurs more readily with α-HHPs or with their precursor, H_2O_2. As well, the reactivity of α-HHPs with the OH radical is likely to be high. Our previous study (Zhao et al., 2012) suggested that a major fraction of formic acid observed during glyoxal photooxidation proceeded via an α-HHP intermediate.

Finally, we note that α-HHPs will likely decompose if aerosol is exposed to the fluid lining the lung, providing a source of reactive oxygen species such as H_2O_2 to the body. In particular, Hasson and Paulson (2003) indicate that the minimum H_2O_2 concentration to cause damage to alveolar cell is likely to be at the order of 0.1 to 1 mM in ALW. Our simulations above suggest that the α-HHP concentration have the potential to be at or above this minimum level.

5 Conclusions

We have investigated the thermodynamics of aqueous-phase formation of α-hydroxyhydroperoxides (α-HHP) arising from H_2O_2 reacting with a suite of atmospherically relevant carbonyl compounds. We find that:

- Formation of α-HHP was significant from many small, atmospherically-relevant aldehydes, but not from methacrolein and ketones.
- Preliminary simulations demonstrate that α-HHP formation will likely be of minor importance in cloud water but is more likely to be of importance in aerosol liquid water where the concentrations of H_2O_2 and aldehydes are higher.
- In ALW, α-HHP may significantly enhance the effective Henry's Law constants of aldehydes and H_2O_2 leading to significant concentrations of α-HHP in solution but probably not affecting the gas-phase levels of these chemicals.
- The levels of α-HHP are likely to be enhanced at lower temperatures.
- α-HHPs can act as nucleophiles to form peroxyhemiacetals.
- In general, this chemistry is likely to lead to higher concentrations of organic peroxides than expected in ALW.

Supplementary material related to this article is available online at: http://www.atmos-chem-phys-discuss.net/13/5509/2013/acpd-13-5509-2013-supplement.pdf.

Acknowledgement. The authors thank NSERC and QEII-GSST for financial support.

References

Allen, J., Balcavage, W., Ramachandran, B., and Shrout, A.: Determination of Henry's law constants by equilibrium partitioning in a closed system using a new in situ optical absorbance method, Environ. Toxicol. Chem., 17, 1216–1221, 1998.

Altieri, K. E., Seitzinger, S. P., Carlton, A. G., Turpin, B. J., Klein, G. C., and Marshall, A. G.: Oligomers formed through in-cloud methylglyoxal reactions: chemical composition, properties, and mechanisms investigated by ultra-high resolution FT-ICR mass spectrometry, Atmos. Environ., 42, 1476–1490, 2008.

Arellanes, C., Paulson, S., Fine, P., and Sioutas, C.: Exceeding of Henry's law by hydrogen peroxide associated with urban aerosols, Environ. Sci. Technol., 40, 4859–4866, 2006.

Atkinson, R.: Gas-phase tropospheric chemistry of organic-compounds – a review, Atmos. Environ. Part A, 24, 1–41, 1990.

Betterton, E. A. and Hoffmann, M. R.: Henry law constants of some environmentally important aldehydes, Environ. Sci. Technol., 22, 1415–1418, 1988.

Bonn, B., von Kuhlmann, R., and Lawrence, M.: High contribution of biogenic hydroperoxides to secondary organic aerosol formation, Geophys. Res. Lett., 31, L10108, 2004.

Bruice, P. Y.: Organic Chemistry, Pearson Education, Upper Saddle River, NJ, 2004.

Carlton, A. G., Turpin, B. J., Altieri, K. E., Seitzinger, S., Reff, A., Lim, H. J., and Ervens, B.: Atmospheric oxalic acid and SOA production from glyoxal: results of aqueous photooxidation experiments, Atmos. Environ., 41, 7588–7602, 2007.

Carter, W., Darnall, K., Graham, R., Winer, A., and Pitts, J.: Reactions of C_2 and C_4 alpha-hydroxy radicals with oxygen, J. Phys. Chem., 83, 2305–2311, 1979.

Chen, Z. M., Wang, H. L., Zhu, L. H., Wang, C. X., Jie, C. Y., and Hua, W.: Aqueous-phase ozonolysis of methacrolein and methyl vinyl ketone: a potentially important source of atmospheric aqueous oxidants, Atmos. Chem. Phys., 8, 2255–2265, doi:10.5194/acp-8-2255-2008, 2008.

Claeys, M., Wang, W., Ion, A., Kourtchev, I., Gelencser, A., and Maenhaut, W.: Formation of secondary organic aerosols from isoprene and its gas-phase oxidation products through reaction with hydrogen peroxide, Atmos. Environ., 38, 4093–4098, 2004.

Docherty, K., Wu, W., Lim, Y., and Ziemann, P.: Contributions of organic peroxides to secondary aerosol formed from reactions of monoterpenes with O_3, Environ. Sci. Technol., 39, 4049–4059, 2005.

Ervens, B. and Volkamer, R.: Glyoxal processing by aerosol multiphase chemistry: towards a kinetic modeling framework of secondary organic aerosol formation in aqueous particles, Atmos. Chem. Phys., 10, 8219–8244, doi:10.5194/acp-10-8219-2010, 2010.

Ervens, B., Turpin, B. J., and Weber, R. J.: Secondary organic aerosol formation in cloud droplets and aqueous particles (aqSOA): a review of laboratory, field and model studies, Atmos. Chem. Phys., 11, 11069–11102, doi:10.5194/acp-11-11069-2011, 2011.

Gab, S., Turner, W., Wolff, S., Becker, K., Ruppert, L., and Brockmann, K.: Formation of alkyl and hydroxyalkyl hydroperoxides on ozonolysis in water and in air, Atmos. Environ., 29, 2401–2407, 1995.

Glushonok, G., Glushonok, T., and Shadyro, O.: Kinetics of equilibrium attainment between molecular glycolaldehyde structures in an aqueous solution, Kinet. Catal., 41, 620–624, 2000.

Greenzaid, P., Luz, Z., and Samuel, D.: A nuclear magnetic resonance study of reversible hydration of aliphatic aldehydes and ketones. I. Oxygen-17 and proton spectra and equilibrium constants, J. Am. Chem. Soc., 89, 749–756, 1967.

Hall, W. A. and Johnston, M. V.: Oligomer formation pathways in secondary organic aerosol from MS and MS/MS measurements with high mass accuracy and resolving power, J. Am. Soc. Mass Spectrom., 23, 1097–1108, 2012.

Hasson, A. and Paulson, S.: An investigation of the relationship between gas-phase and aerosol-borne hydroperoxides in urban air, J. Aerosol Sci., 34, 459–468, 2003.

Hasson, A., Orzechowska, G., and Paulson, S.: Production of stabilized Criegee intermediates and peroxides in the gas phase ozonolysis of alkenes. 1. Ethene, trans-2-butene, and 2,3-dimethyl-2-butene, J. Geophys. Res., 106, 34131–34142, 2001.

Hasson, A., Chung, M., Kuwata, K., Converse, A., Krohn, D., and Paulson, S.: Reaction of Criegee intermediates with water vapor – an additional source of OH radicals in alkene ozonolysis?, J. Phys. Chem. A, 107, 6176–6182, 2003.

He, S. Z., Chen, Z. M., Zhang, X., Zhao, Y., Huang, D. M., Zhao, J. N., Zhu, T., Hu, M., and Zeng, L. M.: Measurement of atmospheric hydrogen peroxide and organic peroxides in Beijing before and during the 2008 Olympic Games: chemical and physical factors influencing their concentrations, J. Geophys. Res., 115, D17307, doi:10.1029/2009JD013544, 2010.

Hellpointner, E. and Gab, S.: Detection of methyl, hydroxymethyl and hydroxyethyl hydroperoxides in air and precipitation, Nature, 337, 631–634, 1989.

Herrmann, H., Hoffmann, D., Schaefer, T., Braeuer, P., and Tilgner, A.: Tropospheric aqueous-phase free-radical chemistry: radical sources, spectra, reaction kinetics and prediction tools, Chem. Phys. Chem., 11, 3796–3822, 2010.

Hewitt, C. and Kok, G.: Formation and occurrence of organic hydroperoxides in the troposphere – laboratory and field observations, J. Atmos. Chem., 12, 181–194, 1991.

Kamboures, M. A., Nizkorodov, S. A., and Gerber, R. B.: Ultrafast photochemistry of methyl hydroperoxide on ice particles, Proc. Natl. Acad. Sci. USA, 107, 6600–6604, 2010.

Kooijman, P. and Ghijsen, W.: Properties and constitution of the peroxides prepared by oxidizing propane and their analysis, J. R. Neth. Chem. Soc., 66, 205–216, 1947.

Kroll, J. H. and Seinfeld, J. H.: Chemistry of secondary organic aerosol: formation and evolution of low-volatility organics in the atmosphere, Atmos. Environ., 42, 3593–3624, 2008.

Lee, M., Heikes, B., and O'Sullivan, D.: Hydrogen peroxide and organic hydroperoxide in the troposphere: a review, Atmos. Environ., 34, 3475–3494, 2000.

Lee, A. K., Zhao, R., Gao, S. S., and Abbatt, J. P.: Aqueous-phase OH oxidation of glyoxal: application of a novel analytical approach employing aerosol mass spectrometry and complementary off-line techniques, J. Phys. Chem. A, 115, 10517–10526, 2011.

Lim, Y. B., Tan, Y., Perri, M. J., Seitzinger, S. P., and Turpin, B. J.: Aqueous chemistry and its role in secondary organic aerosol (SOA) formation, Atmos. Chem. Phys., 10, 10521–10539, doi:10.5194/acp-10-10521-2010, 2010.

Lind, J., Lazrus, A., and Kok, G.: Aqueous phase oxidation of sulfur(IV) by hydrogen-peroxide, methylhydroperoxide, and peroxyacetic acid, J. Geophys. Res., 92, 4171–4177, 1987.

Liu, Y., Monod, A., Tritscher, T., Praplan, A. P., DeCarlo, P. F., Temime-Roussel, B., Quivet, E., Marchand, N., Dommen, J., and Baltensperger, U.: Aqueous phase processing of secondary organic aerosol from isoprene photooxidation, Atmos. Chem. Phys., 12, 5879–5895, doi:10.5194/acp-12-5879-2012, 2012.

Marklund, S.: Simultaneous determination of bis(hydroxymethyl)-peroxide (BHMP), hydroxymethylhydroperoxide (HMP), and H_2O_2 with titanium(IV) – equilibria between peroxides and stabilities of HMP and BHMP at physiological conditions, Acta Chem. Scand., 25, 3517–3531, 1971.

Martin, L. and Damschen, D.: Aqueous oxidation of sulfur-dioxide by hydrogen-peroxide at low pH, Atmos. Environ., 15, 1615–1621, 1981.

Matthews, J., Sinha, A., and Francisco, J.: Unimolecular dissociation and thermochemistry of CH_3OOH, J. Chem. Phys., 122, 221101, doi:10.1063/1.1928228, 2005.

Milas, N. and Golubovic, A.: Studies in organic peroxides. 25. Preparation, separation and identification of peroxides derived from methyl ethyl ketone and hydrogen peroxide, J. Am. Chem. Soc., 81, 5824–5826, 1959a.

Milas, N. and Golubovic, A.: Studies in organic peroxides. 26. Organic peroxides derived from acetone and hydrogen peroxide, J. Am. Chem. Soc., 81, 6461–6462, 1959b.

Monod, A., Chevallier, E., Jolibois, R. D., Doussin, J. F., Picquet-Varrault, B., and Carlier, P.: Photooxidation of methylhydroperoxide and ethylhydroperoxide in the aqueous phase under simulated cloud droplet conditions, Atmos. Environ., 41, 2412–2426, 2007.

Neeb, P., Sauer, F., Horie, O., and Moortgat, G.: Formation of hydroxymethyl hydroperoxide and formic acid in alkene ozonolysis in the presence of water vapour, Atmos. Environ., 31, 1417–1423, 1997.

Ortiz-Montalvo, D. L., Lim, Y. B., Perri, M. J., Seitzinger, S. P., and Turpin, B. J.: Volatility and yield of glycolaldehyde SOA formed through aqueous photochemistry and droplet evaporation, Aerosol Sci. Technol., 46, 1002–1014, 2012.

Perri, M. J., Seitzinger, S., and Turpin, B. J.: Secondary organic aerosol production from aqueous photooxidation of glycolaldehyde: laboratory experiments, Atmos. Environ., 43, 1487–1497, 2009.

Polle, A. and Junkermann, W.: Inhibition of apoplastic and symplastic peroxidase-activity from Norway spruce by the photooxidant hydroxymethyl hydroperoxide, Plant Physiol., 104, 617–621, 1994.

Roehl, C. M., Marka, Z., Fry, J. L., and Wennberg, P. O.: Near-UV photolysis cross sections of CH_3OOH and $HOCH_2OOH$ determined via action spectroscopy, Atmos. Chem. Phys., 7, 713–720, doi:10.5194/acp-7-713-2007, 2007.

Sakugawa, H., Kaplan, I., Tsai, W., and Cohen, Y.: Atmospheric hydrogen-peroxide, Environ. Sci. Technol., 1452–1462, 1990.

Sander, E. G. and Jencks, W. P.: Equilibria for additions to carbonyl group, J. Am. Chem. Soc., 90, 6154, 1968.

Satterfield, C. and Case, L.: Reaction of aldehyde and hydrogen peroxide in aqueous solution – kinetics of the initial reaction, Ind. Eng. Chem., 46, 998–1001, 1954.

Sauer, F., Schuster, G., Schafer, C., and Moortgat, G.: Determination of H_2O_2 and organic peroxides in cloud- and rain-water on the Kleiner Feldberg during FELDEX, Geophys. Res. Lett., 23, 2605–2608, 1996.

Sauer, F., Schafer, C., Neeb, P., Horie, O., and Moortgat, G.: Formation of hydrogen peroxide in the ozonolysis of isoprene and simple alkenes under humid conditions, Atmos. Environ., 33, 229–241, 1999.

Simpson, A. and Brown, S.: Purge NMR: Effective and easy solvent suppression, J. Magn. Reson., 175, 340–346, 2005.

Sorensen, P.: The reversible addition of water to glycolaldehyde in aqueous solution, Acta Chem. Scand., 26, 3357–3365, 1972.

Sorensen, P., Bruhn, K., and Lindelov, F.: Kinetics and equilibria for reversible hydration of aldehyde group in glyoxylic-acid, Acta Chem. Scand. Ser. A, 28, 162–168, 1974.

Stefan, M. I. and Bolton, J. R.: Reinvestigation of the acetone degradation mechanism in dilute aqueous solution by the UV/H_2O_2 process, Environ. Sci. Technol., 33, 870–873, 1999.

Tan, Y., Perri, M. J., Seitzinger, S. P., and Turpin, B. J.: Effects of precursor concentration and acidic sulfate in aqueous glyoxal-OH radical oxidation and implications for secondary organic aerosol, Environ. Sci. Technol., 43, 8105–8112, 2009.

Tan, Y., Carlton, A. G., Seitzinger, S. P., and Turpin, B. J.: SOA from methylglyoxal in clouds and wet aerosols: measurement and prediction of key products, Atmos. Environ., 44, 5218–5226, 2010.

Tang, I., Tridico, A., and Fung, K.: Thermodynamic and optical properties of sea salt aerosols, J. Geophys. Res., 102, 23269–23275, 1997.

Tobias, H. and Ziemann, P.: Thermal desorption mass spectrometric analysis of organic aerosol formed from reactions of 1-tetradecene and O_3 in the presence of alcohols and carboxylic acids, Environ. Sci. Technol., 34, 2105–2115, 2000.

Valverde-Canossa, J., Wieprecht, W., Acker, K., and Moortgat, G.: H_2O_2 and organic peroxide measurements in an orographic cloud: the FEBUKO experiment, Atmos. Environ., 39, 4279–4290, 2005.

Volkamer, R., Ziemann, P. J., and Molina, M. J.: Secondary Organic Aerosol Formation from Acetylene (C_2H_2): seed effect on SOA yields due to organic photochemistry in the aerosol aqueous phase, Atmos. Chem. Phys, 9, 1907–1928, doi:10.5194/acp-9-1907-2009, 2009.

Wallace, T.: Quantitative-analysis of a mixture by NMR-spectroscopy, J. Chem. Educ., 61, 1074–1074, 1984.

Wang, H. L., Huang, D., Zhang, X., Zhao, Y., and Chen, Z. M.: Understanding the aqueous phase ozonolysis of isoprene: distinct product distribution and mechanism from the gas phase reaction, Atmos. Chem. Phys., 12, 7187–7198, doi:10.5194/acp-12-7187-2012, 2012.

Wasa, T. and Musha, S.: Polarographic behavior of glyoxal and its related compounds, Bull. Univ. Osaka Prefect. Set. A, 19, 169–180, 1970.

Yaylayan, V., Harty-Majors, S., and Ismail, A.: Investigation of the mechanism of dissociation of glycolaldehyde dimer (2,5-dihydroxy-1,4-dioxane) by FTIR spectroscopy, Carbohydr. Res., 309, 31–38, 1998.

Yee, L. D., Craven, J. S., Loza, C. L., Schilling, K. A., Ng, N. L., Canagaratna, M. R., Ziemann, P. J., Flagan, R. C., and Seinfeld, J. H.: Secondary organic aerosol formation from low-NO_x photooxidation of dodecane: evolution of multigeneration gas-phase chemistry and aerosol composition, J. Phys. Chem. A, 116, 6211–6230, 2012.

Yu, G., Bayer, A., Galloway, M., Korshavn, K., Fry, C., and Keutsch, F.: Glyoxal in aqueous ammonium sulfate solutions: products, kinetics and hydration effects, Environ. Sci. Technol., 45, 6336–6342, 2011.

Zhao, R., Lee, A. K. Y., and Abbatt, J. P. D.: Investigation of aqueous-phase photooxidation of glyoxal and methylglyoxal by aerosol chemical ionization mass spectrometry: observation of hydroxyhydroperoxide formation, J. Phys. Chem. A, 116, 6253–6263, 2012.

Zhou, X. and Lee, Y.: Aqueous solubility and reaction-kinetics of hydroxymethyl hydroperoxide, J. Phys. Chem., 96, 265–272, 1992.

Zhou, X. and Mopper, K.: Apparent partition-coefficients of 15 carbonyl-compounds between air and seawater and between air and fresh water – implications for air sea exchange, Environ. Sci. Technol., 24, 1864–1869, 1990.

Ziemann, P. J. and Atkinson, R.: Kinetics, products, and mechanisms of secondary organic aerosol formation, Chem. Soc. Rev., 41, 6582–6605, 2012.

Table 1. Summary of hydration equilibrium constants (K_{hyd}) measured by NMR. The constants are reported with their standard deviation arising from the number of replicates indicated on the table.

	NMR (this work)		Literature[a]
	K_{hyd}	# replicates	K_{hyd}
Formaldehyde	> 18[b]	14	2.3×10^3 [1]
Acetaldehyde	1.43 ± 0.04	15	1.43 [2]
Propionaldehyde	1.26 ± 0.13	16	0.7 [2]
Glycolaldehyde	16.0 ± 1.3	16	10 [3] 17.5[c] [4]
Methacrolein	< 0.005[b]	16	–
Glyoxal	p.o.[d]	16	2.2×10^5 [5]
Methylglyoxal	> 57 ± 155[b]	16	2.3×10^3 [5]
Glyoxylic acid	> 18[b]	16	3000 [6]
Acetone	< 0.002[b]	2	0.002 [7]
Methylethyl ketone	< 0.005[b]	6	–

[a] References used: [1] Betterton and Hermann (1988); [2] Greenzaid et al. (1967); [3] Sorensen (1972); [4] Yaylayan et al. (1998); [5] Wasa and Musha (1970); [6] Sorensen (1974); [7] Bruice et al. (2004).
[b] Calculated using the limit of quantification of the current methods.
[c] In D_2O.
[d] p.o.: Values could not be determined due to peaks overlapping with the H_2O peak.

Table 2. Summary of the apparent equilibrium constants of α-HHP formation (K_{app}) measured and reported in literature at 25 °C. The constants are reported with their standard deviation acquired from the number of replicates shown on the table.

	NMR measurement			PTR-MS measurement			Literature[a]
	K_{app} (M^{-1})	# Replicates	Catalase recovery (%)	K_{app} (M^{-1})	# Replicates	Catalase recovery (%)	K_{app} (M^{-1})
Formaldehyde	164 ± 31[b]	12	p.o.[c]	n.p.[d]	n.p.	n.p.	126 [1] 150 [2] 94 [3]
Acetaldehyde	94.8 ± 12.5	11	97 ± 1	132 ± 15	8	95.8	48 [3]
Propionaldehdye	51.1 ± 8.0	12	83 ± 3	84 ± 12	8	85	–
Glycolaldehyde	43.3 ± 3.9	12	89 ± 4	n.p.	n.p.	n.p.	–
Methacrolein	0.8 ± 0.7	12	n.p.	n.d.[e]	6	n.p.	–
Glyoxal	p.o.	12	p.o.	n.p.	n.p.	n.p.	40–200 [4]
Methylglyoxal	25 ± 4[f]	12	85[g]	n.p.	n.p.	n.p.	40–200 [4]
Glyoxylic acid	440 ± 270[f]	13	78[g]	n.p.	n.p.	n.p.	–
Acetone	< 0.008[h]	2	n.p.	n.d.	6	n.p.	–
Methylethyl ketone	< 0.02[h]	6	n.p.	n.d.	4	n.p.	–

[a] References used: [1] Marklund (1972); [2] Zhou and Lee (1992); [3] Kooijiman and Ghijsen (1947); [4] Zhao et al. (2012).
[b] Including the formation of BHMP (see text).
[c] p.o.: Values could not be determined due to peaks overlapping with the H_2O peak.
[d] n.p.: Experiment not performed.
[e] n.d. Not detected at the current detection limit of PTR-MS.
[f] A significant amount of formic acid was observed. The K_{app} value is determined with the consideration of irreversible formic acid formation.
[g] A decreasing trend of the recovery with increasing concentration of H_2O_2 addition.
[h] Calculated using the limit of quantification of the current methods.

Table 3. Temperature dependence of the apparent equilibrium constant (K_{app}) of 1-hydroxyethyl hydroperoxide (1-HEHP) formation from acetaldehyde.

Temperature (°C)	K_{app} (M^{-1})	# Replicates
25	132 ± 15	12
15	206 ± 40	6
5	311 ± 38	8

Table 4. Effects of inorganic salt addition on the hydration equilibrium constant (K_{hyd}) and the apparent α-HHP formation equilibrium constant (K_{app}).

	Acetaldehyde			Glycolaldehyde		
Experiment	K_{hyd} and K_{app} (M^{-1})	# Replicates	p-value	K_{hyd} and K_{app} (M^{-1})	# Replicates	p-value
No Salt	K_{hyd} 1.43 ± 0.04	15	–	K_{hyd} 16.0 ± 1.3	16	–
	K_{app} 94.8 ± 12.5	11	–	K_{app} 43.3 ± 3.9	12	–
1 M	K_{hyd} 1.48 ± 0.07	4	0.11	K_{hyd} 17.8 ± 0.3	3	4.3×10^{-5}[a]
$(NH_4)_2SO_4$	K_{app} 81.3 ± 12.7	3	4.0×10^{-3}[a]	K_{app} 35.6 ± 2.4	3	9.7×10^{-5}[a]
1 M	K_{hyd} 1.58 ± 0.04	3	0.10	K_{hyd} 18.5 ± 0.5	3	3.8×10^{-3}[a]
Na_2SO_4	K_{app} 82.3 ± 10.0	3	0.072	K_{app} 30.8 ± 2.4	3	4.8×10^{-4}[a]

[a] Statistically significant at the 95 % confidence level (p-value < 0.05).

Table 5. Conditions assumed in the atmospheric partitioning simulation of 1 ppb of aldehydes or H_2O_2.

	Cloud water	Aerosol liquid water (ALW)
Temperature	25 C°	25 C°
Atmospheric pressure	1 atm	1 atm
Liquid water content (LWC)	1 g m^{-3}	1 µg m^{-3}
Aqueous-phase H_2O_2	100 µM	10 mM
Aqueous-phase total aldehyde	100 µM	100 mM

Table 6. Results of the atmospheric partitioning simulation.

		Formaldehyde		Acetaldehyde		H_2O_2	
		Cloud water	ALW	Cloud water	ALW	Cloud water	ALW
Without α-HHP formation	K_H[a] (M atm^{-1})	3.0×10^3		17		7.10×10^4	
	Gas-phase mixing ratio (ppb)	0.932	1.000	1.000	1.000	0.366	1.000
	Fraction in aqueous phase	0.068	7.33×10^{-8}	4.15×10^{-4}	4.15×10^{-10}	0.634	1.74×10^{-6}
	K_{app} (M^{-1})	164		113[b]		100[c]	
With α-HHP formation	K_{Heff} (M atm^{-1})	3.05×10^3	7.92×10^3	17	36	7.17×10^4	7.81×10^5
	Gas-phase mixing ratio (ppb)	0.931	1.000	1.000	1.000	0.363	1.000
	Fraction in aqueous phase	6.93×10^{-2}	1.94×10^{-7}	4.20×10^{-4}	8.86×10^{-10}	0.637	1.91×10^{-5}
	Aqueous-phase total α-HHP (M)	4.27×10^{-8}	4.92×10^{-6}	1.92×10^{-10}	1.92×10^{-8}	9.43×10^{-9}	7.1×10^{-4}

[a] References: formaldehyde (Betterton and Hoffmann, 1988); acetaldehyde (Zhou and Mopper, 1990); H_2O_2 (Martin and Damschen, 1981).
[b] Value taken from the current work as the average of the NMR results and the PTR-MS results.
[c] Value assumed as the average K_{app} for α-HHP from all the aldehyde species.

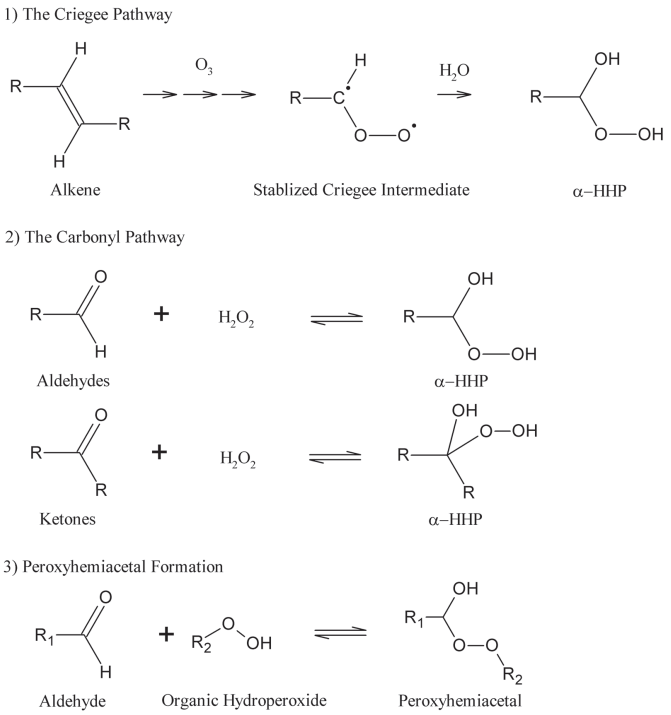

Fig. 1. Two aqueous-phase pathways of *α*-hydroxyhydroperoxide (*α*-HHP) formation: (1) the Criegee Pathway, (2) the Carbonyl pathway, and a related reaction (3) peroxyhemiacetal formation.

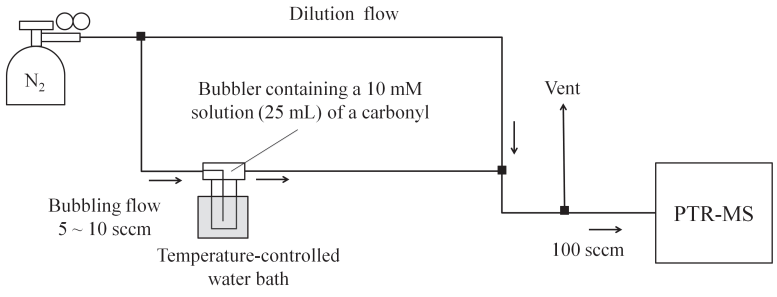

Fig. 2. Experimental setup for the PTR-MS measurements.

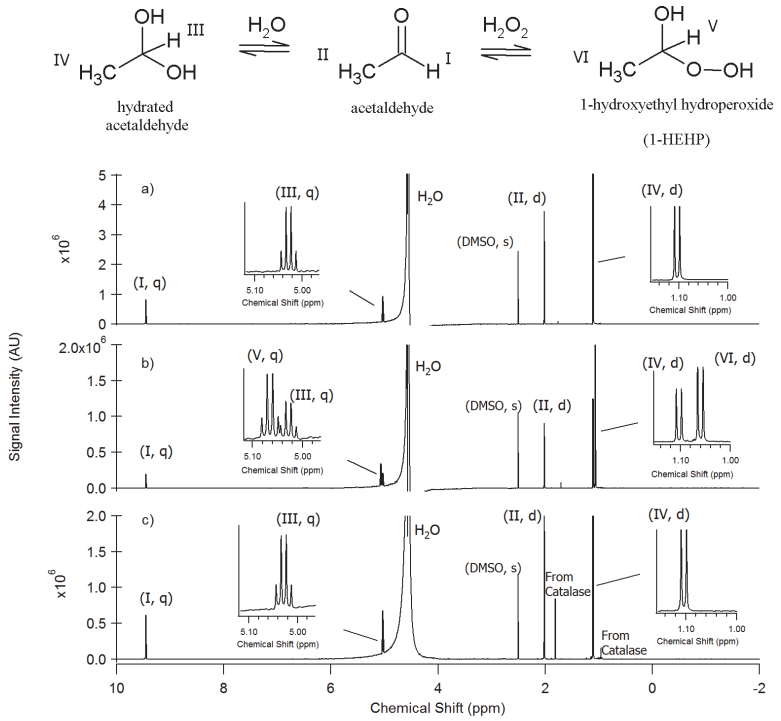

Fig. 3. ^{1}H NMR spectra for acetaldehyde. **(a)** Acetaldehyde aqueous solution; **(b)** 17.7 mM of H_2O_2 was added to the acetaldehyde solution; **(c)** catalase was added to the solution to quench H_2O_2. The insets are the magnified view of certain regions of the spectra. The split pattern and the identity of each peak are shown in the brackets (the numbers match those in the chemical structures).

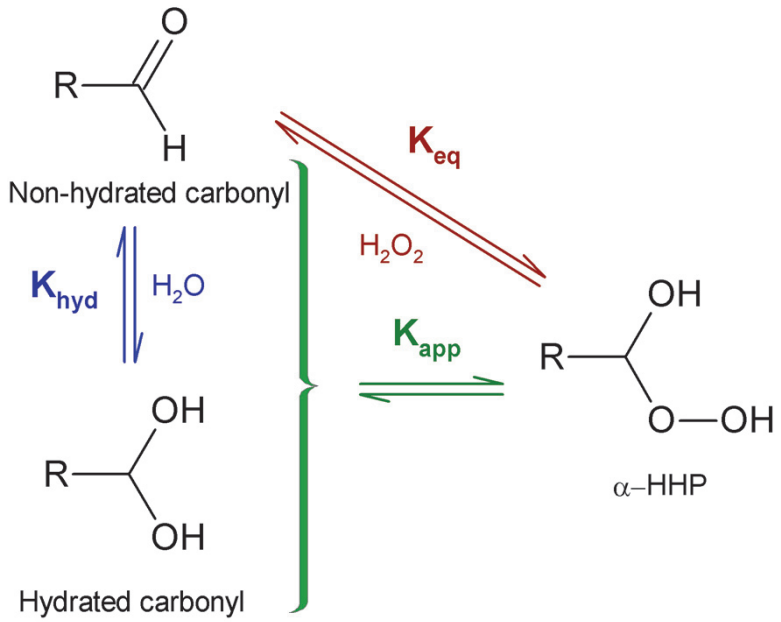

Fig. 4. Hydration equilibrium constant (K_{hyd}), the α-HHP formation equilibrium constant (K_{eq}) and the apparent α-HHP formation equilibrium constant (K_{app}). Please see the text for details.

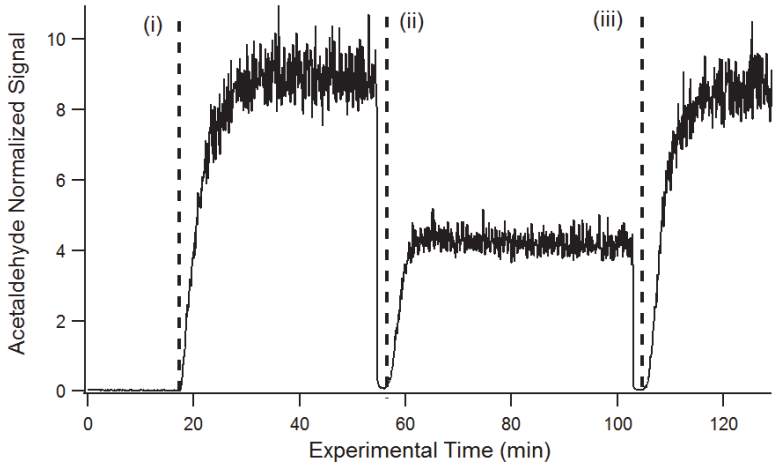

Fig. 5. Sample time series of signal due to gas-phase acetaldehyde in the PTR-MS experiment. The acetaldehyde signal normalized to the reagent ion is shown as a function of time. Time (i): 25 mL of clean water in the bubbler is replaced by 25 mL of acetaldehyde solution (10 mM), time (ii): 13.3 mM of H_2O_2 is added to the acetaldehyde solution, time (iii): one drop of catalase stock solution is added.

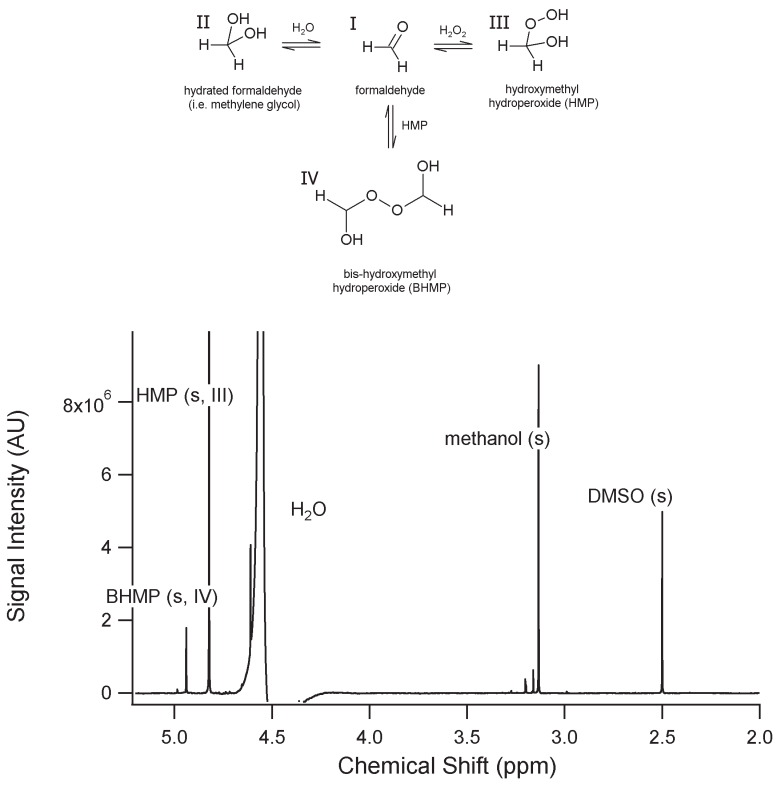

Fig. 6. ^{1}H NMR spectra of a formaldehyde-H_2O_2 mixture. The splitting pattern and assignment of the peaks are shown in the bracket.

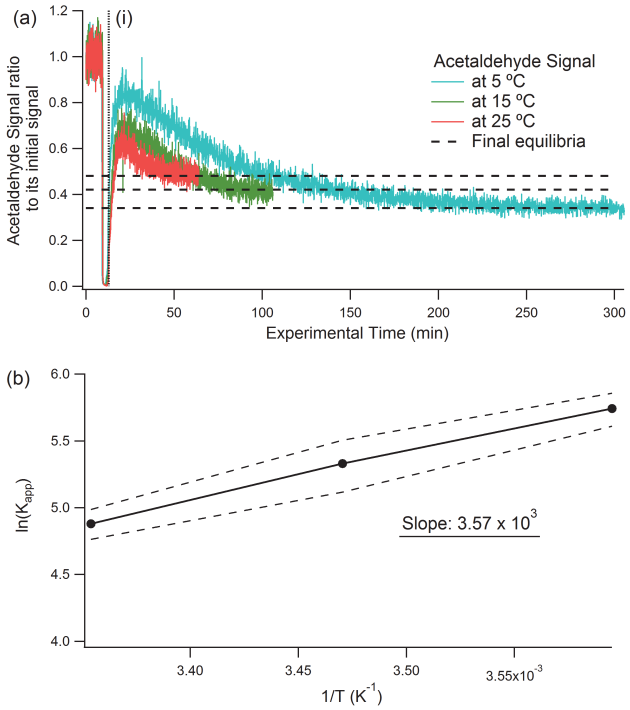

Fig. 7. Typical acetaldehyde time profiles at 5, 15 and 25 °C are shown in **(a)**. The ratios of signal at a given time to the initial signal are shown. H_2O_2 (13.3 mM) was injected to the 10 mM acetaldehyde solutions at time (i). The dashed lines show the signal levels at equilibrium. The van't Hoff diagram for 1-hydroxyethyl hydroperoxide (1-HEHP) formation from acetaldehyde is shown in **(b)**. The dashed lines connects $+1\sigma$ and -1σ from the average $\ln(K_{app})$ determined at the three temperatures.

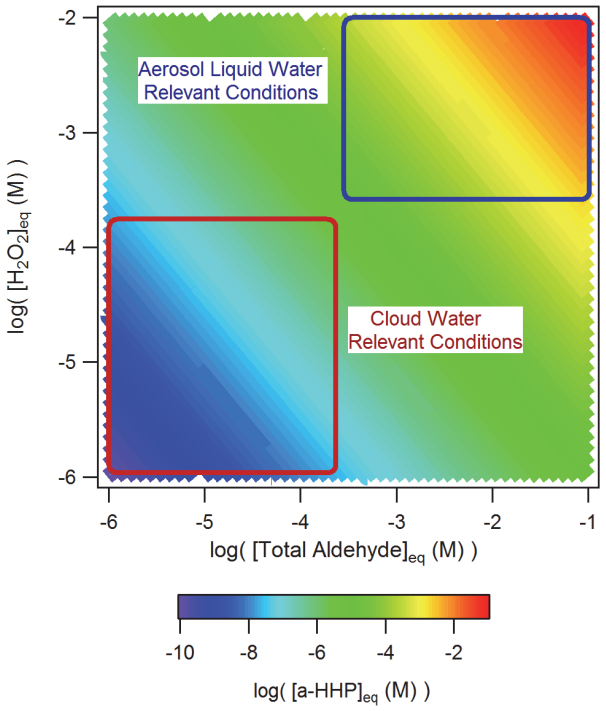

Fig. 8. Simulation of the equilibrium concentration of α-hydroxyhydroperoxide ($[\alpha\text{-HHP}]_{eq}$) arising from various equilibrium concentrations of H_2O_2 ($[H_2O_2]_{eq}$) and total aldehyde ($[\text{Total Aldehyde}]_{eq}$). The concentrations are all presented in log scale. Conditions relevant to cloud water and aerosol water are also indicated. This simulation considers α-HHP formation via only the Carbonyl Pathway, with an average equilibrium constant of 100 M^{-1}.

Discussion Paper | Discussion Paper | Discussion Paper | Discussion Paper |